

radiative rates from their $^1(d\sigma^*p\sigma)$ states.

The strong ΔA increase at 440 nm for the $^1A_{2u}$ state of $Rh_2(TMB)_4^{2+}$ is expected for a $^1(d\sigma^*p\sigma)$ electronic configuration. The strength of the 440-nm band and its shape are very similar to those of related complexes, all of which exhibit intense $d\sigma^* \rightarrow p\sigma$ absorptions. That this $d\sigma^* \rightarrow p\sigma$ transition in the $^1A_{2u}$ state of $Rh_2(TMB)_4^{2+}$ is to the blue of its location in the ground state ($^1A_{1g} \rightarrow ^1A_{2u}$, $\lambda_{max} = 515$ nm) may be due to spin-pairing and electronic polarization differences between these two states. In particular, the $d\sigma^* \rightarrow p\sigma$ transition in $Rh_2(TMB)_4^{2+}$ unpairs two electrons, creating half-filled $d\sigma^*$ and $p\sigma$ orbitals, while the $d\sigma^* \rightarrow p\sigma$ transition in the $^1A_{2u}$ state both pairs two electrons in the $p\sigma$ orbital and leaves an empty $d\sigma^*$ orbital at lower energy. Importantly, the strong 440-nm band in the ΔA spectrum of the $^1A_{2u}$ state of $Rh_2(TMB)_4^{2+}$ does not have a counterpart in the spectrum of the $^3A_{2u}$ state. The formation of a $^1(p\sigma)^2$ electronic configuration as a result of a $d\sigma^* \rightarrow p\sigma$ transition should be much less allowed from the $^3A_{2u}$ state. Thus, the spectral results on $Rh_2(TMB)_4^{2+}$ are consistent with prior assignments of the two lowest-energy excited states in d^8-d^8 complexes.¹

The unobservably short lifetime ($\tau < 20$ ps) of the 1B_2 state of Ir_2 accords with its low fluorescence quantum yield but contrasts with the 820-ps lifetime of the $^1A_{2u}$ state of $Rh_2(TMB)_4^{2+}$. This trend is consistent with the greater spin-orbit coupling expected for the iridium dimer,¹¹ but a quantitative comparison is not feasible because of the significant structural differences between the two Rh and Ir complexes.

Although the fluorescence quantum yield of the 1B_2 state of Ir_2 decreases by 30% in DCE relative to its yield in nonreactive cyclohexane, the yield of the 3B_2 state is the same in these two solvents. Additionally no evidence of photochemical reaction as a result of 1B_2 quenching is seen in the 360-500-nm difference

spectrum during the first 11 ns after photoexcitation. Reasonable conclusions are that (1) there is no significant oxidative addition photochemistry proceeding from the 1B_2 state and (2) the reduced fluorescence yield in DCE is due to slightly more rapid intersystem crossing in this solvent than in cyclohexane. This is not likely to be due to an external heavy-atom effect as is commonly found for organic molecules; rather it more likely reflects a solvent-specific interaction. Since DCE modifies neither the absorption nor the emission spectrum of Ir_2 , the interaction between the metal complex and the chlorinated hydrocarbon solvent is likely to be weak. Inasmuch as Ir_2 has two vacant coordination sites and haloalkanes are known to be weak bases,¹² a weak Lewis acid-base pairing of the two molecules is plausible. This interaction could sufficiently perturb the electronic and vibrational structure of Ir_2 to produce a 30% increase in the rate of intersystem crossing in haloalkanes vs. alkanes.

This work has shown that the 3B_2 state of Ir_2 is populated extremely rapidly, indicating that photochemistry from upper excited states is not likely. Similarly, extraneous energy losses from nonreactive, nonradiative processes also appear to be insignificant prior to the formation of the 3B_2 state. The observation that a decrease in 1B_2 fluorescence in DCE relative to cyclohexane did not produce a change in the yield of the 3B_2 state suggests that the quantum yield for formation of this state is near unity.

Acknowledgment. This research was carried out at Brookhaven National Laboratory under Contract DE-AC02-76H00016 with the US Department of Energy and supported by its Division of Chemical Sciences, Office of Basic Energy Sciences. Research at the California Institute of Technology was supported by National Science Foundation Grant CHE84-19828. We thank Dr. V. M. Miskowski for providing us with the $Rh_2(TMB)_4^{2+}$ complex and for helpful discussions.

Registry No. $Rh_2(TMB)_4^{2+}$, 73367-41-6; $[Ir(\mu-pz)(COD)]_2$, 80462-13-1.

(12) Smith, C. F.; Chandrasekhar, J.; Jorgensen, W. L. *J. Phys. Chem.* **1982**, *86*, 3308-3318 and references therein.

(10) (a) Rice, S. F. Ph.D. Dissertation, California Institute of Technology, Pasadena, 1982. (b) Thomas, T. R.; Crosby, G. A. *J. Molec. Spectrosc.* **1971**, *38*, 118-129. (c) Felix, F.; Ferguson, J.; Gudel, H. U.; Ludi, A. *J. Am. Chem. Soc.* **1980**, *102*, 4096-4102.

(11) Figgis, B. N. "Introduction to Ligand Fields"; Interscience: New York, 1966.

Rhenium Carbonyl Biradicals. Formation, Recombination, and Halogen Atom Transfer¹

Kang-Wook Lee, John M. Hanckel, and Theodore L. Brown*

Contribution from the School of Chemical Sciences, University of Illinois at Urbana—Champaign, Urbana, Illinois 61801. Received August 12, 1985

Abstract: The organometallic biradicals $\cdot(OC)_4ReL\widehat{L}Re(CO)_4$ ($L\widehat{L} = R_2P(CH_2)_nPR_2$; R = Me, Ph, Cy; $n = 2-6$ or *cis*- $Ph_2PCH=CHPh_2$) have been observed as transient species following laser flash photolysis of the bridging ligand substituted dirhenium octacarbonyls, in which homolytic metal-metal bond cleavage is a dominant primary photoprocess and CO dissociation is negligible. The intramolecular recombination of these biradicals follows simple first-order kinetics. The rate constants for recombination show a slight solvent dependence probably related to viscosity and the sizes of solvent molecules. The rate constants are affected by steric requirements of the substituents on phosphorus atoms and geometry in the ligand backbone. The rate constants for halogen atom transfer to the biradicals, determined either by laser flash photolysis or by continuous photolysis, are characteristic of mononuclear rhenium carbonyl radicals with similar substituent environments. The metal-centered biradicals thus show typical monoradical behavior in their reactions such as recombination, halogen atom transfer, and electron transfer.

In recent years there has been much interest in transition-metal-centered radicals generated by flash photolysis. Various metal carbonyl dimers including $M_2(CO)_8L_2$ (M = Mn, Re; L = CO, PR_3 , AsR_3) are known to undergo both metal-metal bond

homolysis and CO dissociation following irradiation at wavelengths corresponding to a $\sigma \rightarrow \sigma^*$ or $d\pi \rightarrow \sigma^*$ transition.²⁻¹² The radicals

(1) This research was supported by the National Science Foundation through Research Grant NSF CHE 83-12331.

(2) Wrighton, M. S.; Ginley, D. S. *J. Am. Chem. Soc.* **1975**, *97*, 2065.

(3) (a) Hepp, A. F.; Wrighton, M. S. *J. Am. Chem. Soc.* **1983**, *105*, 5934.

(b) *Ibid.* **1981**, *103*, 1258.

(4) Freedman, A.; Bersohn, R. *J. Am. Chem. Soc.* **1978**, *100*, 4116.

(5) Leopold, D. G.; Vajda, V. *J. Am. Chem. Soc.* **1984**, *106*, 3720.

yields $(\mu\text{-H})\text{Re}_2(\text{CO})_8(\mu\text{-CH}=\text{CHC}_4\text{H}_9)$. Reflux of the crude $(\mu\text{-H})\text{Re}_2(\text{CO})_8(\mu\text{-CH}=\text{CHC}_4\text{H}_9)$ in methylene chloride in the presence of a bidentate phosphine ligand (LL) for 6–24 h gives the desired compound as a major product (at least 60% isolated yield) except where LL is dpph. The crude product, $\text{Re}_2(\text{CO})_8(\mu\text{-L}\text{L})$, was washed with hexane 3 times to remove the unreacted $\text{Re}_2(\text{CO})_{10}$ and $(\mu\text{-H})\text{Re}_2(\text{CO})_8(\mu\text{-CH}=\text{CHC}_4\text{H}_9)$ and then with a 3:1 hexane/ethylacetate mixture 3 times to remove most of the unreacted bidentate phosphine ligand. The pure product was isolated on a column or by preparative thin-layer chromatography with hexane and methylene chloride followed by recrystallization with the same solvent system. The analytical and spectroscopic data for $\text{Re}_2(\text{CO})_8(\mu\text{-L}\text{L})$ are listed in Table I.

Halogen Atom Transfer. The photochemical reaction of $\text{Re}_2(\text{CO})_8(\mu\text{-dppp})$ (0.085 g, 0.084 mmol) in toluene (15 mL) in the presence of CCl_4 (1 mL) or CH_2Br_2 (1 mL) was carried out for 1 h with a GE 275-W sunlamp to yield $\text{X}(\text{CO})_4\text{RePPh}_2(\text{CH}_2)_3\text{Ph}_2\text{PRe}(\text{CO})_4\text{X}$ ($\text{X} = \text{Cl}$ or Br). The isolated yield was ~80%. $\text{Cl}(\text{OC})_4\text{RePPh}_2(\text{CH}_2)_3\text{Ph}_2\text{PRe}(\text{CO})_4\text{Cl}$: IR (toluene) ν_{CO} 2105 (w), 2008 (s), 1998 (s), 1931 (m, br) cm^{-1} and (CCl_4) ν_{CO} 2106 (w), 2018 (s), 1998 (vs), 1942 (m, br) cm^{-1} . FDMS M^+ at m/e 1084 based on ^{187}Re and ^{37}Cl (the highest peak = 1080). Anal. Calcd: C, 38.93; H, 2.43; Cl, 6.57; P, 5.74. Found: C, 38.85; H, 2.47; Cl, 6.94; P, 6.46. $\text{Br}(\text{OC})_4\text{RePPh}_2(\text{CH}_2)_3\text{Ph}_2\text{PRe}(\text{CO})_4\text{Br}$: IR (CCl_4) ν_{CO} 2106 (w), 2018 (m), 2001 (s), 1995 (m, sh), 1943 (m, br) cm^{-1} .

Electron Transfer. Photolysis of $\text{Re}_2(\text{CO})_8(\text{PMe}_3)_2$ in acetonitrile in the presence of $\text{C}_7\text{H}_7^+\text{BF}_4^-$ at ambient temperature leads to $[\text{Re}(\text{CO})_4(\text{PMe}_3)(\text{NCMe})]^+\text{BF}_4^-$ (IR (CH_3CN) ν_{CO} 2123 (w), 2035 (m, sh), 2022 (s), 1987 (m), 1938 (w) cm^{-1}).^{17b} The corresponding reaction of $\text{Re}_2(\text{CO})_8(\mu\text{-dppp})$ shows new IR peaks at 2123 (w), 2037 (m, sh), 2022 (s), 1983 (m), and 1937 (w) cm^{-1} , which are very similar in pattern to those for $[\text{Re}(\text{CO})_4(\text{PMe}_3)(\text{NCMe})]^+$. Fast atom bombardment mass spectrum exhibits $(M - 87)^+$ at m/e 1179. On the basis of these spectroscopic data the product was assigned to $[(\text{MeCN})(\text{OC})_4\text{RePPh}_2(\text{CH}_2)_3\text{Ph}_2\text{PRe}(\text{CO})_4(\text{NCMe})]^{2+}2\text{BF}_4^-$.

Kinetics Techniques. The laser flash photolysis apparatus has been described previously.¹⁶ All reactions were carried out under a N_2 or Ar atmosphere and at ambient temperature (20–24 °C).

Samples for laser flash photolysis were prepared in a drybox and loaded into a 25-mL round-bottomed flask connected to a 1.00 cm path length quartz cuvette by glass tubing. The entire sample container was sealed with a threaded Teflon stopcock. Sample solutions, 2×10^{-4} – 5×10^{-4} M in dirhenium carbonyls, were freeze-pump-thaw degassed 3 times and then sealed under argon at ambient temperature prior to flash photolysis. Sample solutions, 1.0×10^{-2} – 1.3×10^{-2} M in $\text{Re}_2(\text{CO})_8(\mu\text{-dppp})$, for continuous photolysis were loaded into a CaF₂ IR cell in a N_2 glovebox. A GE 275-W sunlamp was used as a source.

Data collection was begun 30 ns or more following the flash pulse to avoid tailing from the laser pulse. The data were analyzed in terms of a first-order rate law by least-squares fits of $\ln(\text{absorbance})$ vs. time. Data through the first two or more half-lives were employed. All reported rate constants are the means of values from 3–5 experiments, each having linear least-squares correlation coefficients greater than 0.98 for recombination and 0.94 for halogen atom transfer. The predicted ranges (μ) for the rate constants were calculated from the following equation: $\mu = \sigma_{n-1}t(n)^{-1/2}$ where σ_{n-1} is the standard deviation, t is the t score for a 95% level of certainty, and n is the number of samples. Data for continuous photolysis were collected for the first 15–30% of reaction. The observed zero-order rate constants were obtained by least-squares fits of absorbance vs. time.

Results and Discussion

Fluxional Behavior of $\text{Re}_2(\text{CO})_8(\mu\text{-L}\text{L})$ ($\text{L}\text{L} = \text{dppe}, \text{dppp}, \text{dppb}$). It has been reported that $\text{Re}_2(\text{CO})_8(\mu\text{-dppe})$ undergoes a fluxional process on the NMR time scale, in which the orientation of two equatorially coordinated phosphorus atoms is rapidly exchanged between two staggered conformations with respect to the Re–Re bond.²³ A similar process occurs for $\text{Re}_2(\text{CO})_8(\mu\text{-dppp})$ and $\text{Re}_2(\text{CO})_8(\mu\text{-dppb})$. The ¹³C NMR spectrum of $\text{Re}_2(\text{CO})_8(\mu\text{-dppb})$ in the carbonyl region at ambient temperature, which shows three sharp peaks [204.3 (d, 4 C, $J_{\text{PC}} = 3.9$ Hz), 193.9 (d, 2 C, $J_{\text{PC}} = 48.2$ Hz), 190.9 (d, 2 C, $J_{\text{PC}} = 8.1$ Hz)], corresponds to the average of two staggered conformations. As the temperature is lowered, the peak at 204.3 ppm is broadened (–58 °C) and splits into two peaks at –94 °C (δ 205.6 and 201.3). The free energies of activation for exchange (ΔG_c^\ddagger), estimated

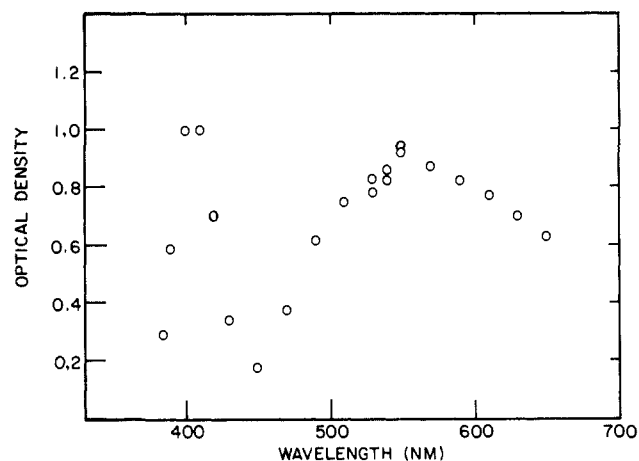
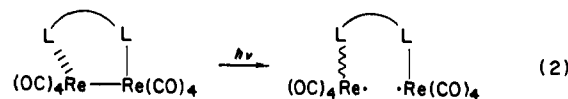


Figure 1. Absorbance spectrum of $(\text{OC})_4\text{RePCy}_2(\text{CH}_2)_2\text{Cy}_2\text{PRe}(\text{CO})_4$ biradical reported as a plot of $A_0 - A_\infty$ vs. wavelength.

from the coalescence temperature and the peak separation in the low-temperature limit, are 12.3, 11.0, and 9.6 kcal/mol for $\text{Re}_2(\text{CO})_8(\mu\text{-dppe})$, $\text{Re}_2(\text{CO})_8(\mu\text{-dppp})$, and $\text{Re}_2(\text{CO})_8(\mu\text{-dppb})$, respectively.²⁴ Clearly, the intramolecular rotational process associated with the exchange becomes more facile as the number of methylene groups in the ligand backbone increases. Darensbourg and co-workers²⁵ have reported the molecular structure of $[(\mu\text{-H})\text{Mo}_2(\text{CO})_8(\mu\text{-dppb})]^-$ in which the two phosphorus atoms of dppb are oriented in the staggered conformation about the Mo–Mo bond. Our results indicate that the most stable conformation in $\text{Re}_2(\text{CO})_8(\mu\text{-R}(\text{CH}_2)_n\text{PR}_2)$ ($n = 2\text{--}6$) is also the staggered form.

Metal-Centered Biradical Formation. Photolysis of $\text{Re}_2(\text{CO})_8(\mu\text{-Ph}_2\text{PCH}_2\text{PPh}_2)$ in the presence of CCl_4 has been reported to give the chlorine atom abstracted compound, $\text{Cl}(\text{OC})_4\text{RePPh}_2\text{CH}_2\text{Ph}_2\text{PRe}(\text{CO})_4\text{Cl}$ (eq 1).²⁰ The corresponding reactions of $\text{Re}_2(\text{CO})_8(\mu\text{-L}\text{L})$ ($\text{L}\text{L} = \text{dppe}, \text{dppb}, \text{dcype}$) also yield $\text{Cl}(\text{OC})_4\text{ReL}\text{LRe}(\text{CO})_4\text{Cl}$, as discussed later. These results indicate that biradicals, $(\text{OC})_4\text{ReL}\text{LRe}(\text{CO})_4$, are probably formed by photolysis of $\text{Re}_2(\text{CO})_8(\mu\text{-L}\text{L})$.

Laser flash photolysis (337 nm) of decalin solutions of $\text{Re}_2(\text{CO})_8(\mu\text{-L}\text{L})$ ($\text{L}\text{L} = \text{dmpe}, \text{dppe}, \text{dcype}, \text{dppp}, \text{dppb}, \text{dppe}$, dpph, or *cis*- $\text{Ph}_2\text{PCH}=\text{CHPPh}_2$) gives rise to transient absorption spectra in the 540-nm region. Decays of transients within 1 μs follow first-order kinetics and are unaffected by the presence of CO in solution. The lifetimes of the $(\sigma)^1(\sigma^*)^1$ excited states of $\text{M}_2(\text{CO})_{10}$ ($\text{M} = \text{Mn}, \text{Re}$) are observed to be shorter than 25 ps;^{6,19a} thus the observed absorption in the time domain 30 ns–1 μs appears to be due to biradicals, $(\text{OC})_4\text{ReL}\text{LRe}(\text{CO})_4$, formed as in eq 2. The approximate positions of λ_{max} for the



$(\text{OC})_4\text{RePCy}_2(\text{CH}_2)_2\text{Cy}_2\text{PRe}(\text{CO})_4$ biradical (405 and 550 nm), located by measurement of optical density ($A_0 - A_\infty$) 30 ms after the flash vs. λ (385 nm to 650 nm) as shown in Figure 1, are in good agreement with the values in the ranges 400–410 and 540–560 nm found for metal-centered rhenium carbonyl radicals.^{9,17,26}

Vaida and co-workers⁵ and Kobayashi et al.¹² have recently proposed that CO dissociation is comparatively more important in the flash photolysis of $\text{Re}_2(\text{CO})_{10}$ than for $\text{Mn}_2(\text{CO})_{10}$. The magnitude of the transient absorption observed at 380 nm (λ_{max} for $\text{Re}_2(\text{CO})_7\text{L}_2$) following laser flash photolysis of a 1,2-diax-

(23) Lee, K.-W.; Pennington, W. T.; Cordes, A. W.; Brown, T. L. *Organometallics* 1984, 3, 404.

(24) Calculations of ΔG_c^\ddagger were reported elsewhere: Lee, K.-W.; Brown, T. L. *Organometallics* 1985, 4, 1025.

(25) Darensbourg, M. Y.; El Mehdaoui, R.; Delord, T. J.; Fronczek, F. R.; Watkins, S. F. *J. Am. Chem. Soc.* 1984, 106, 2583.

(26) Walker, H. W.; Rattinger, G. B.; Belford, R. L.; Brown, T. L. *Organometallics* 1983, 2, 775.

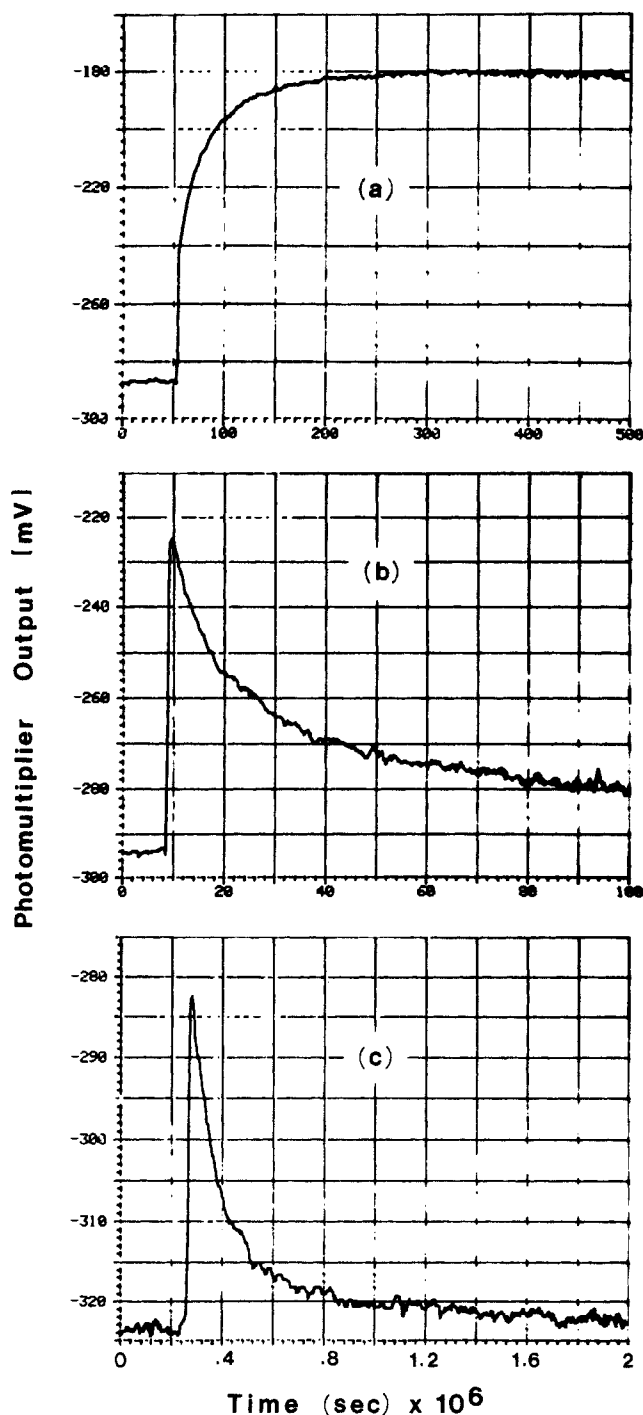


Figure 2. Photomultiplier outputs (mV) upon laser flash photolysis of (a) 1,2-djax- $\text{Re}_2(\text{CO})_8(\text{PCy}_3)_2$ in hexane at 380 nm, (b) 1,2-dieq- $\text{Re}_2(\text{CO})_8[\text{P}(\text{O}-i\text{-Pr})_3]_2$ in hexane at 385 nm, and (c) 1,2-dieq- $\text{Re}_2(\text{CO})_8(\mu\text{-dppb})$ in decalin at 400 nm. The absorption in each case is the sum of the absorption due to (1) The radical (or biradical); (2) $\text{Re}_2(\text{CO})_7\text{L}_2$; (3) $\text{Re}_2(\text{CO})_8\text{L}_2$. In (a) only (2) and (3) contribute significantly; in (b) only (1) and (2); in (c) only (1).

$\text{Re}_2(\text{CO})_8\text{L}_2$ ($\text{L} = \text{PPh}_2\text{Et}, \text{PCy}_3$) solution shows that $\text{Re}_2(\text{CO})_7\text{L}_2$ is produced in substantial amounts as a photoproduct (Figure 2a), indicating that CO dissociation is a significant process. The increase in absorption in Figure 2a during the first 200 μs is due to absorption by $\text{Re}_2(\text{CO})_8\text{L}_2$, which is formed by radical-radical recombination. The absorbance seen after 200 μs following the flash, as compared with the preflash level, is ascribable entirely to $\text{Re}_2(\text{CO})_7(\text{PCy}_3)_2$. On a longer time scale the absorbance returns to the base line as recombination with CO occurs. The transient absorption spectrum observed at 385 or 420 nm following flash photolysis of 1,2-dieq- $\text{Re}_2(\text{CO})_8\text{L}_2$ [$\text{L} = \text{P}(\text{O}-i\text{-Pr})_3, \text{PMe}_3$]

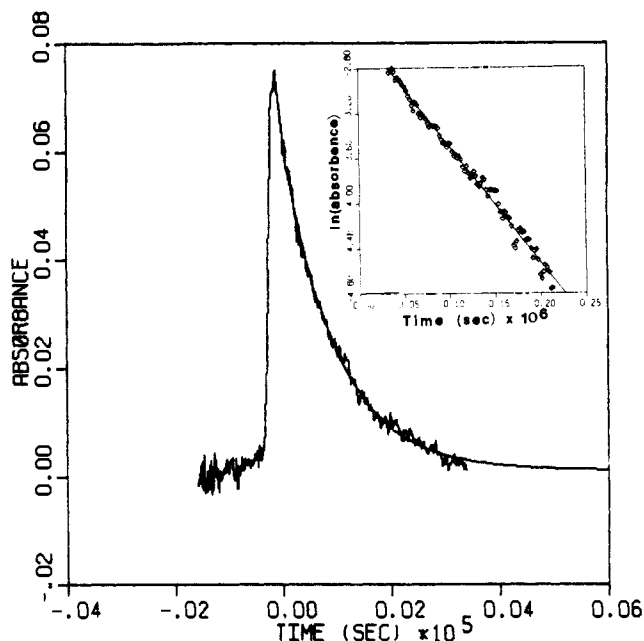


Figure 3. Change in absorbance vs. time at 540 nm on laser flash photolysis of a solution of $\text{Re}_2(\text{CO})_8(\mu\text{-dppb})$ in decalin (3×10^{-4} M) under an argon atmosphere. The line through the trace represents the first-order least-squares fit of the data for disappearance of the transient. Insert: linear least-squares fit of the data to a first-order rate law expression.

(Figure 2b) shows that the transient absorption due to the radical is more intense than that due to longer-lived $\text{Re}_2(\text{CO})_7\text{L}_2$ or due to $\text{Re}_2(\text{CO})_8[\text{P}(\text{O}-i\text{-Pr})_3]_2$ being formed, so there is a decline from an initially high absorbance as the radicals recombine. The absorbance remaining at 100 μs and longer as compared with the preflash level is due to the CO dissociated product $\text{Re}_2(\text{CO})_7[\text{P}(\text{O}-i\text{-Pr})_3]_2$. Clearly, this absorbance is much smaller than in $\text{Re}_2(\text{CO})_7(\text{PCy}_3)_2$ (Figure 2a). A very low transient absorption due to $\text{Re}_2(\text{CO})_7(\mu\text{-L})\text{L}$ is observed in the range 380–430 nm following photolysis of $\text{Re}_2(\text{CO})_8(\mu\text{-L})\text{L}$ compounds (Figure 2c). We conclude that CO loss to form $\text{Re}_2(\text{CO})_7(\mu\text{-L})\text{L}$ is a very minor photochemical pathway. The ratio of CO dissociation to homolytic metal-metal bond cleavage thus apparently decreases in the order 1,2-diax- $\text{Re}_2(\text{CO})_8\text{L}_2 > 1,2\text{-dieq-}\text{Re}_2(\text{CO})_8\text{L}_2 > 1,2\text{-dieq-}\text{Re}_2(\text{CO})_8(\mu\text{-L})\text{L}$.

Rates of Recombination of $\cdot(\text{OC})_4\text{ReL}(\text{L})\text{Re}(\text{CO})_4\cdot$ Biradicals. Solutions of $\text{Re}_2(\text{CO})_8(\mu\text{-L})\text{L}$ were subjected to laser flash photolysis with the monitor monochromator set at the wavelength of the absorbance maximum (540–550 nm) for the biradical. The absorbance usually returns to its original value. The decay of the transient follows first-order kinetics, as shown in Figure 3. The values obtained for the rate constants are not affected by the change in wavelength at which data are taken in the range 470–610 nm. These results suggest that the recombination of biradicals is intramolecular. The IR spectrum taken after 1000 or more flashes with frequent shakings of the cell shows only the starting material. In the absence of added atom donor reagents there is no evidence for intermolecular cross-couplings or other reactions of the biradicals. Table II contains the measured first-order recombination rate constants, k_2 . The recombination rate constants are affected by two steric factors: substituents on phosphorus atoms and geometry in the ligand backbone. In the recombinations of $\cdot\text{Mn}(\text{CO})_4(\text{PR}_3)$ radicals, the rate constants are affected mainly by steric factors.^{11a} Among biradicals derived from the dmpe, dppe, and dcype compounds, the k_2 values decrease in the order dmpe > dppe > dcype. The Corey-Pauling-Koltun (CPK) molecular models of those biradicals indicate that bulkier groups on phosphorus push the metal-bound CO ligands toward the other metal center, causing repulsions between the CO groups on the two metal atoms.

The substantial difference in k_2 values for the $\text{Ph}_2\text{PCH}_2\text{CH}_2\text{PPh}_2$ and *cis*- $\text{Ph}_2\text{PCH}=\text{CHPPh}_2$ compounds (2.8

Table II. Recombination Rate Constants of $\cdot(\text{OC})_4\text{ReL}\widehat{\text{L}}\text{Re}(\text{CO})_4\cdot$ Biradicals

$\widehat{\text{L}}\text{L}^a$	solvent	$k_2 \times 10^{-7}, \text{s}^{-1}$	lifetime, ^c ns
dmpe	decalin	8.1 ± 0.1	12
dppe	decalin	2.8 ± 0.2	36
dcype	decalin	0.34 ± 0.01	290
	tetralin	0.48 ± 0.03	210
	mesitylene	0.62 ± 0.03	160
	toluene	0.77 ± 0.02	130
	benzyl alcohol	0.72 ± 0.02	140
	THF	2.2 ± 0.1	45
cis-dppet	decalin	0.75 ± 0.02	130
dppp	decalin	2.8 ± 0.3	36
dppb	decalin (3.4) ^b	1.0 ± 0.0	97
	tetralin (2.2)	1.7 ± 0.2	60
	mesitylene	2.8 ± 0.2	36
	toluene (0.59)	2.4 ± 0.1	42
	benzene (0.65)	2.4 ± 0.1	42
	THF (0.55)	3.6 ± 0.2	28
	acetonitrile (0.37)	>10	<10
dppe	decalin	1.5 ± 0.1	67
dpph	decalin	1.2 ± 0.3	87

^admpe = $\text{Me}_2\text{P}(\text{CH}_2)_2\text{PMe}_2$; dppe = $\text{Ph}_2\text{P}(\text{CH}_2)_2\text{PPh}_2$; dcype = $\text{C}_6\text{H}_5\text{P}(\text{CH}_2)_2\text{PCy}_2$; dppet = $\text{Ph}_2\text{PCH}=\text{CHPPh}_2$; dppp = $\text{Ph}_2\text{P}(\text{CH}_2)_3\text{PPh}_2$; dppb = $\text{Ph}_2\text{P}(\text{CH}_2)_4\text{PPh}_2$; dpppe = $\text{Ph}_2\text{P}(\text{CH}_2)_5\text{PPh}_2$; dpph = $\text{Ph}_2\text{P}(\text{CH}_2)_6\text{PPh}_2$. ^bValues in parentheses are solvent viscosities in centipoise at 25 °C. ref: Šedivec, V.; Filek, J. *Handbook of Analysis of Organic Solvents*; Ellis Horwood Ltd., England, 1976. ^cLifetime refers to the reciprocal of the rate constant for transient decay and corresponds to the time required for the concentration to decay to e^{-1} ($1/2.728$) of its initial value.

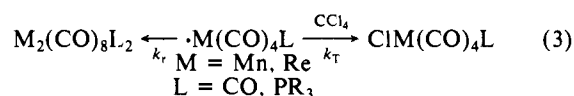
$\times 10^7 \text{ s}^{-1}$ vs. $0.75 \times 10^7 \text{ s}^{-1}$) probably also has its origin in steric factors. Molecular models indicate that the intramolecular ring in the *cis*- $\text{Ph}_2\text{PCH}=\text{CHPPh}_2$ compound is more strained than in the $\text{Ph}_2\text{PCH}_2\text{CH}_2\text{PPh}_2$ compound. The existence of that strain is likely to lead to some activation energy requirement for reforming the metal-metal bond; the biradical corresponding to the *cis*- $\text{Ph}_2\text{PCH}=\text{CHPPh}_2$ compound thus has a longer lifetime, despite the fact that the metal centers are constrained to remain in close proximity.

The variation in wavelength of the absorption assignable to the $\sigma \rightarrow \sigma^*$ transition lends some support to the argument that internal ring strain or strain due to interligand repulsions accounts for at least some of the variation in the barrier to recombination. In the series involving the $\text{Ph}_2\text{P}(\text{CH}_2)_n\text{PPh}_2$ ligands, the k_2 values are higher for $n = 2$ ($\lambda_{\text{max}} = 336 \text{ nm}$) and 3 ($\lambda_{\text{max}} = 342 \text{ nm}$) than for $n = 4, 5$, or 6 ($\lambda_{\text{max}} = 358, 363$, and 356 nm , respectively). The existence of an internal ring strain contributing to a weakening of the metal-metal bond might well be manifested in increased values for λ_{max} .²⁷ Similarly, in the series $\text{R}_2\text{P}(\text{CH}_2)_2\text{PR}_2$, λ_{max} is 334, 336, and 342 nm for $\text{R} = \text{CH}_3, \text{C}_2\text{H}_5, \text{C}_6\text{H}_{11}$, respectively. Once again, it might be plausibly argued that increased interligand repulsion is responsible for the increase in λ_{max} . This is also the order of decreasing recombination rate constant.

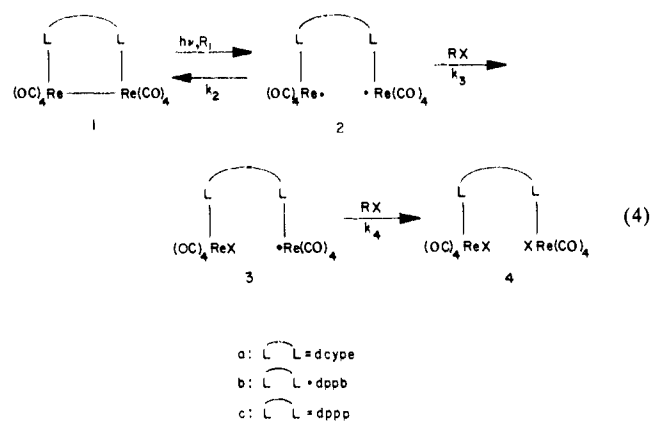
The k_2 values for the $\text{Re}_2(\text{CO})_8(\text{dppb})$ biradical exhibit an interesting solvent dependence. The lifetime of organic biradicals generated in the Norrish type II reaction is observed to depend on stabilization resulting from hydrogen bonding with solvent.²⁸ However, in the present case there are no functional groups on the radicals capable of significant hydrogen bonding with the solvent. As shown in Table II there is a general increase in k_2 as solvent viscosity decreases. The observed relationship of k_2 to solvent viscosity suggests that solvent molecules intrude to some extent between the two rhenium centers in the biradical. In such a situation the recombination rate might be expected to depend on the ease with which the solvent molecule can be extruded from the intervening space, which in turn should relate at least crudely

to macroscopic solvent viscosity. However, it is also possible that the viscosity is a measure of the rate at which the hot biradical generated in the primary photoprocess is capable of thermally equilibrating with its solvent surroundings. If this rate is slower in the more viscous medium because of slower energy diffusion away from the solute cavity, there may be more opportunity for the biradical to undergo torsional motions that cause the radical centers to be further apart in the thermalized product biradical.

Rates of Halogen Atom Transfer to $\cdot(\text{OC})_4\text{ReL}\widehat{\text{L}}\text{Re}(\text{CO})_4\cdot$ Biradicals. We have reported that the reaction of $\cdot\text{M}(\text{CO})_4\text{L}$ ($\text{M} = \text{Mn}, \text{Re}; \text{L} = \text{CO}, \text{PR}_3$) and CCl_4 is first order in $[\text{CCl}_4]$ over a concentration range 0.06–0.28 or 0.02–0.12 $\text{M}^{16,17}$ and that recombination of the carbonyl radicals makes an insignificant contribution to the transient decay of $\cdot\text{M}(\text{CO})_4\text{L}$ over a $[\text{RX}]$ range 0.02–0.18 M. For the instance of the reaction of $\cdot\text{Mn}(\text{CO})_4\text{P}(n\text{-Bu})_3$ and CCl_4 where k_r is $1.0 \times 10^8 \text{ M}^{-1} \text{ s}^{-1}$, k_T is $1.8 \times 10^6 \text{ M}^{-1} \text{ s}^{-1}$, and $[\cdot\text{M}(\text{CO})_4\text{L}]$ is less than 10^{-6} M (eq 3), the



ratio of recombination rate to halogen atom transfer rate, which can be expressed as $k_r[\cdot\text{Mn}(\text{CO})_4\text{L}]^2/k_T[\text{CCl}_4][\cdot\text{Mn}(\text{CO})_4\text{L}]$, is smaller than 3×10^{-3} when $[\text{CCl}_4] = 0.02 \text{ M}$. However, when $[\text{CCl}_4]$ is low enough, recombination can compete with halogen atom transfer.²⁹ Because the intramolecular recombination rate of $\cdot(\text{OC})_4\text{ReL}\widehat{\text{L}}\text{Re}(\text{CO})_4\cdot$ biradicals is so fast, it competes much more effectively with the bimolecular halogen transfer for a comparable range of donor concentration. Continuous photolysis of $\text{Re}_2(\text{CO})_8(\mu\text{-L})_2$ in the presence of a halogen atom donor such as CCl_4 or CH_2Br_2 leads to halogen atom abstracted compounds, $\text{X}(\text{OC})_4\text{ReL}\widehat{\text{L}}\text{Re}(\text{CO})_4\text{X}$ ($\text{X} = \text{Cl}, \text{Br}$), as a result of successive halogen atom transfers to the biradicals as outlined in eq 4.



The transient absorption spectra from laser flash photolysis of $\text{Re}_2(\text{CO})_8(\mu\text{-L})_2$ ($\widehat{\text{L}}\text{L} = \text{dcype}, \text{dppb}$) in the presence of an appropriate concentration of RX show a pseudo-first-order decay with a time constant shorter than that characteristic of recombination for $[\text{RX}]$ on the order of 0.1 M or greater. The steady-state approximation (appendix) leads to the rate equation

$$k_{\text{obsd}} = \left(\frac{2k_3}{2 + (k_3/k_4)} \right) [\text{RX}] + \left(\frac{2k_2}{2 + (k_3/k_4)} \right) \quad (5)$$

As shown in Figure 4, the observed pseudo-first-order rate constant (k_{obsd}) varies linearly with $[\text{RX}]$ over the range 0.05–0.25 M. k_3 and k_4 can be calculated from eq 5 with use of the slope, y intercept, and knowledge of k_2 . These values are listed in Table III. The k_3 and k_4 values for dcype and dppb biradicals (2a and 2b) are compared with the rate constants of halogen atom transfer for $\cdot\text{Re}(\text{CO})_4[\text{P}(i\text{-Pr})_3]$ and $\cdot\text{Re}(\text{CO})_4(\text{PPh}_2\text{Et})$, respectively (Table III), since the cone angle characteristic of the coordinated

(27) (a) Jackson, R. A.; Poë, A. *Inorg. Chem.* **1978**, *17*, 997. (b) *Ibid.* **1979**, *18*, 3331.

(28) (a) Scajano, J. C. *Acc. Chem. Res.* **1982**, *15*, 252. (b) Hrovat, D. A.; Lju, J. H.; Turro, N. J.; Weiss, R. G. *J. Am. Chem. Soc.* **1984**, *106*, 7033. (c) Scajano, J. C. *Tetrahedron*, **1982**, *38*, 819. (d) Wilson, R. M. In *Organic Photochemistry*, Padwa, A., Ed.; Marcel Dekker: New York, **1985**.

(29) (a) Fox, A.; Poë, A. *J. Am. Chem. Soc.* **1980**, *102*, 2497. (b) Laine, R. M.; Ford, P. C. *Inorg. Chem.* **1977**, *16*, 388.

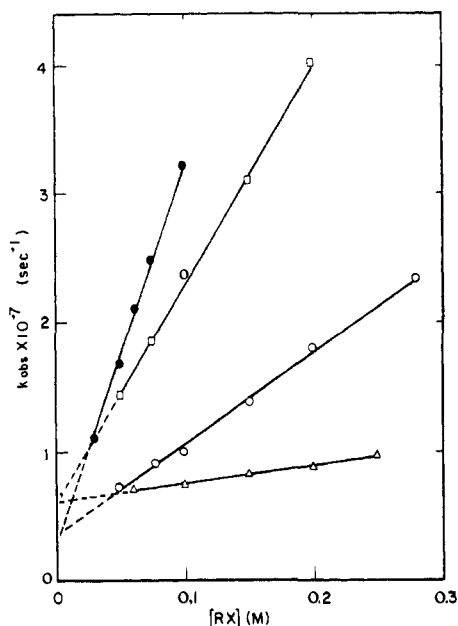


Figure 4. Variation in k_{obs} with $[\text{RX}]$ in the reaction of the $\text{Re}_2(\text{CO})_8(\text{L-L})$ biradical with RX : (●), L-L = dppb, $\text{RX} = \text{CCl}_4$; (□), L-L = dppb, $\text{RX} = \text{CH}_2\text{Br}_2$; (○), L-L = dcype, $\text{RX} = \text{CCl}_4$; (Δ), L-L = dcype, $\text{RX} = \text{CH}_2\text{Br}_2$.

Table III. Rate Constants for Halogen Atom Transfer^a

compound	halogen atom donor	k_3	k_4	k_T	k_3/k_4
2a	CCl_4	1.6×10^8	6.5×10^7		2.4
	CH_2Br_2	1.8×10^7	3.3×10^7		0.56
2b	CCl_4	9.3×10^8	2.1×10^8		4.5
	CH_2Br_2	2.9×10^8	2.0×10^8		1.5
2c	CCl_4	5.4×10^8			
	CH_2Br_2	2.2×10^8			
$\cdot\text{Re}(\text{CO})_4\text{-}[\text{P}(i\text{-Pr})_3]_3^b$	CCl_4			9.3×10^7	
	CH_2Br_2			1.4×10^7	
$\cdot\text{Re}(\text{CO})_4\text{-}(\text{PPh}_2\text{Et})$	CCl_4			5.8×10^8	
	CH_2Br_2			2.1×10^8	

^aUnit of rate constants is $\text{M}^{-1} \text{s}^{-1}$. ^bFrom ref 17.

phosphorus of dcype or dppb is expected to be close to that for $\text{P}(i\text{-Pr})_3$ or PPh_2Et , respectively. k_3 and k_4 are extraordinarily close to the corresponding k_T value in each case.

If each rhenium radical center of the biradical **2** or monoradical **3** had the same rate constant for reaction with a given atom donor, the k_3/k_4 ratio would be 2. The observed ratios in reaction of **2a** with CCl_4 or CH_2Br_2 are 2.4 or 0.56, respectively, and for reaction of **2b** with CCl_4 or CH_2Br_2 they are 4.5 or 1.5, respectively. These are not far from a value of 2. Steric factors will play an important role in determining the specific rate constant in each case. However, the fact that k_3/k_4 is not greatly different from 2 indicates that the inherent reactivity of the rhenium radical centers in the biradical and monoradical are not substantially different, in keeping with the conclusion based on other lines of evidence.

We are unable to determine the k_3 and k_4 values for **2c** since decay of the transient absorption is too fast to permit evaluation of the rate constant with our laser apparatus (15 ns pulse width). However, a value for k_3 can be determined by continuous photolysis. The photolytic reaction of **1c** and CCl_4 or CH_2Br_2 in toluene was carried out in a 0.2 mm CaF_2 IR cell. The rate of disappearance of **1c** measured by IR spectroscopy is constant within the first 15–30% reaction. The zero-order rate constants (k_0) were determined from the relationship between absorbance vs. time. The k_2 value in toluene for $\text{Re}_2(\text{CO})_8(\mu\text{-dppp})$ was estimated to be $6.4 \times 10^7 \text{ s}^{-1}$ from the known recombination rate constants of **2b** in decalin and in toluene and of **2c** in decalin,

assuming that the rate of k_2 in toluene to k_2 in decalin is the same for **2b** and **2c**. Since $R_1 = (\phi I_a)$ in eq 4 should be much smaller than k_2 and k_3 in sunlamp photolysis, it is reasonable to assume that the concentration of **2c** is time independent. This steady-state approximation (Appendix) leads to the rate equation

$$k_0^{-1} = \left(\frac{k_2}{R_1 k_3} \right) [\text{RX}]^{-1} + \left(\frac{1}{R_1} \right) \quad (6)$$

As shown in Figure 5, the inverse of the observed zero-order rate constant, k_0^{-1} , varies linearly with $[\text{RX}]^{-1}$ over a concentration range 0.066–0.28 M. k_3 can be calculated from eq 6 by using the slope, y intercept, and k_2 ; we obtain $5.4 \times 10^8 \text{ M}^{-1} \text{ s}^{-1}$ for CCl_4 and $2.2 \times 10^8 \text{ M}^{-1} \text{ s}^{-1}$ for CH_2Br_2 . These halogen atom transfer rate constants are compared with those of $\cdot\text{Re}(\text{CO})_4(\text{PPh}_2\text{Et})$, $5.8 \times 10^8 \text{ M}^{-1} \text{ s}^{-1}$ for CCl_4 and $2.1 \times 10^8 \text{ M}^{-1} \text{ s}^{-1}$ for CH_2Br_2 , respectively. At the high and low concentration extremes the data depart from the regression line. At low concentration, k_0 is greater than expected probably because of a side reaction. At high concentration, $>0.28 \text{ M}$ in the case of CCl_4 , the approximations underlying eq 6 are invalid. The expected linear relationship obtains for a much higher CH_2Br_2 concentration range (0.28–1.0 M). It is possible in this case that k_2 becomes smaller as $[\text{CH}_2\text{Br}_2]$ increases. We have seen that k_2 decreases with increasing solvent viscosity and solvent molecular mass. CH_2Br_2 is more massive than C_7H_8 and the viscosity of CH_2Br_2 (1.0 cP) is greater than that of toluene (0.59 cP). Therefore, k_2 probably decreases as the concentration of CH_2Br_2 increases.

Electron Transfer of Biradicals. Photolysis of $\text{Re}_2(\text{CO})_8(\mu\text{-dppp})$ in acetonitrile in the presence of $\text{C}_7\text{H}_7^+\text{BF}_4^-$ at ambient temperature leads to $[(\text{MeCN})(\text{OC})_4\text{RePPh}_2(\text{CH}_2)_3\text{Ph}_2\text{PR}(\text{CO})_4(\text{NCMe})]^{2+} \cdot 2\text{BF}_4^-$. These reactions are believed to involve an outer sphere electron transfer from the biradical intermediate. Electron-transfer reactions of this type are known for mononuclear carbonyl radicals.^{3,17b}

Conclusions

The systems described in this contribution represent the first reported examples of organometallic biradicals that are analogous to widely studied organic biradicals such as those formed in the Norrish type II photoprocess,^{28a} i.e., biradicals that lack a direct bonding link between the spin centers. We know very little about the electronic states of the transient biradicals, but at least some conclusions can be drawn from the several observations reported. The observation of absorption maxima in the wavelength range characteristic of that for mononuclear rhenium radicals suggests that the spin centers are not strongly coupled. This conclusion is further reinforced by the rate data for chlorine and bromine atom transfers. The rate constants are remarkably close to those observed for mononuclear rhenium radical centers with analogous steric properties. Analogous behavior is observed for organic biradicals.³⁰

What factors are most important in determining the lifetimes of the biradicals? Among the factors that might be important are intersystem crossing to the singlet manifold; intramolecular torsional motion about one or more bonds in the bidentate phosphine backbone; internal ring strain; interligand repulsions, and interactions with the solvent. Intersystem crossing is not likely to be important, given that the spins are largely centered on heavy metal atoms. We have alluded to the likely influence of the other factors in our discussions of the comparative rates of decay of the transients. The range of recombination rates is not great, a factor of 24 from largest to smallest, so there is no convincing basis at this time on which to distinguish the various contributions to a given rate constant. In general, however, the major factors responsible for the variations in values of k_2 seem to be steric in origin.

(30) (a) Encinas, M. V.; Wagner, P. J.; Scajano, J. C. *J. Am. Chem. Soc.* **1980**, *102*, 1357. (b) Wagner, P. J.; Zepp, R. G. *J. Am. Chem. Soc.* **1972**, *94*, 287. (c) Wagner, P. J.; Kelso, P. A.; Zepp, R. G. *J. Am. Chem. Soc.* **1972**, *94*, 7480.

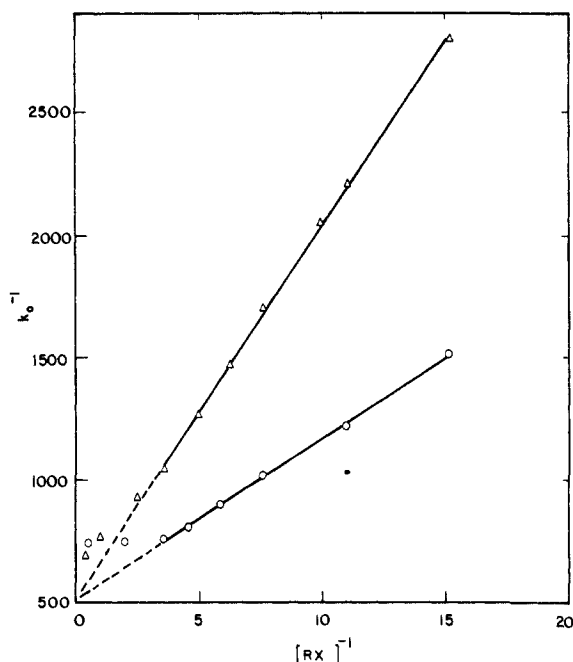


Figure 5. Variation in k_0 with $[RX]$ in the continuous photolysis of $Re_2(CO)_8(\mu\text{-dppp})$ with CCl_4 (O) or CH_2Br_2 (Δ).

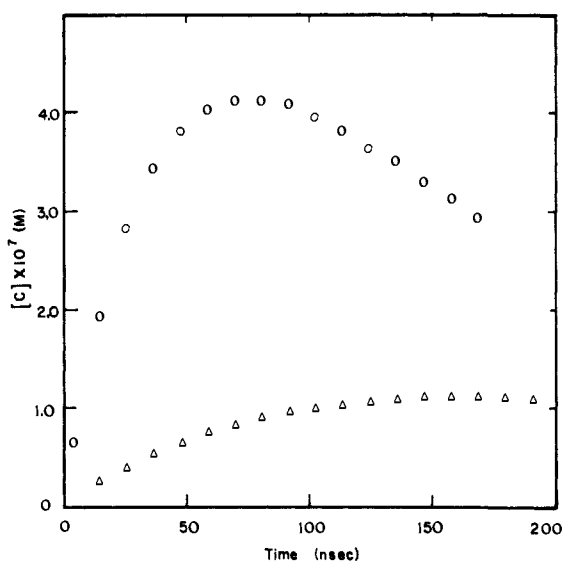


Figure 6. Variation in $[C]$ with time by simulation of the reaction of $Re_2(CO)_8(\mu\text{-dcypr})$ biradical with CCl_4 (O) or CH_2Br_2 (Δ).

It is evident from this work that the biradicals, though comparatively short-lived, nevertheless exhibit some of the same chemical characteristics as the analogous mononuclear radicals. Further, we have shown that CO loss is an inefficient primary photoprocess in these systems as compared with Re-Re bond homolysis. It is now well-established that mononuclear metal carbonyl radical centers are quite labile toward substitution. There is as yet no evidence for lability toward substitution at the metal centers in the biradicals. There are in fact no rate constant data available for substitution at mononuclear $Re(CO)_4L$ radicals, but they are likely to be a few orders of magnitude lower than for substitution into $Re(CO)_5$.¹³ Assuming a bimolecular rate constant for substitution on the order of $10^6 M^{-1} s^{-1}$, substitution at the metal centers in the $Re_2(CO)_8(\mu-L)_2$ compounds under continuous photolysis is expected to be quite slow. The observed photochemical reactions of the $Re_2(CO)_8(\mu-L)_2$ compounds with substrates such as alcohols,²³ alkenes,³¹ and alkynes²⁰ which take place comparatively slowly may thus be occurring via Re-Re bond

homolysis, substitution at the metal radical centers, followed by subsequent reactions to yield the observed products.

Acknowledgment. High-field NMR facilities were provided by the National Science Foundation (NSF Grant CHE 79-16100). High-resolution mass spectrometer facilities were supported in part by a grant from the National Institute of General Medicine Sciences (GM 27029). The ZAB-HF mass spectrometer was purchased in part with grants from the Division of Research Resources, National Institutes of Health (RR 01575), and the National Science Foundation (PCM 8121494).

Appendix

Derivation of Eq 5. For the mechanism in eq 4 let $A = 1$, $B = 2$, $C = 3$, and $D = 4$. Let the absorbing unit in the decay be the individual Re centers, denoted as $Re\cdot$. We assume that all $Re\cdot$ give rise to the same extinction coefficient for absorption at the monitor wavelength. Then,

$$-d[Re\cdot]/dt = k_{obsd}[Re\cdot] \quad (1a)$$

$$-d[B]/dt = k_2[B] + k_3[RX][B] \quad (2a)$$

$$-d[C]/dt = -k_3[RX][B] + k_4[RX][C] \quad (3a)$$

Invoking the steady-state approximation for $[C]$ we can write

$$-d[C]/dt = 0 = -k_3[RX][B] + k_4[RX][C] \quad (4a)$$

$$[C] = (k_3/k_4)[B] \quad (5a)$$

The disappearance rate of $Re\cdot$ can be expressed as in eq 6a

$$-d[Re\cdot]/dt = -(2d[B]/dt + d[C]/dt) \quad (6a)$$

From eq 1a, 2a, 4a, and 6a

$$k_{obsd}[Re\cdot] = 2k_2[B] + 2k_3[RX][B] \quad (7a)$$

$$\text{since } [Re\cdot] = 2[B] + [C]$$

$$k_{obsd}(2[B] + [C]) = 2k_2[B] + 2k_3[RX][B] \quad (8a)$$

Inserting the expression for eq 5a into eq 8a one obtains

$$k_{obsd}\{2[B] + (k_3/k_4)[B]\} = 2k_2[B] + 2k_3[RX][B] \quad (9a)$$

$$k_{obsd} = \left(\frac{2k_2}{2 + (k_3/k_4)} \right) + \left(\frac{2k_3}{2 + (k_3/k_4)} \right)[RX] \quad (5)$$

Justification of the Steady-State Assumption. Variation in the concentration of C with time can be calculated by simulation of the reaction system by using a modification³² of the Havchm program.³³ The input parameters are k_2 , k_3 , k_4 , $[RX]$, $[B]$, and time scale. The concentration of B is assumed to be $10^{-6} M$; the value chosen for this parameter is not of importance to the result. The $[C]$ vs. time relationship is shown in Figure 6. During the time (40–150 ns) we used for calculation of k_{obsd} , the change in $[C]$ is small. Therefore, our steady-state assumption is reasonable.

Derivation of Equation 6. For the mechanism in eq 4 let $A = 1$, $B = 2$, and $C = 3$. Continuous photolysis corresponds to a set of conditions in which the recombination process is much faster than atom transfer. We thus establish a photostationary pre-equilibrium involving A and B . Then,

$$-d[A]/dt = R_1 - k_2[B] \quad (10a)$$

$$d[B]/dt = R_1 - k_2[B] - k_3[B][RX] \quad (11a)$$

Invoking the steady-state approximation

$$d[B]/dt = 0 = R_1 - k_2[B] - k_3[B][RX] \quad (12a)$$

From eq 12a

$$[B] = \frac{R_1}{k_2 + k_3[RX]} \quad (13a)$$

(32) Herrinton, T. R. Ph.D. Thesis, University of Illinois, Urbana, IL, 1984.

(33) Stabler, R. N.; Chesick, J. P. *Int. J. Chem. Kinet.* **1978**, *10*, 461.

(31) Lee, K.-W.; Brown, T. L. *Organometallics* **1985**, *4*, 1030.

The rate of disappearance of A can also be expressed as in eq 14a

$$-d[A]/dt = k_0 \quad (14a)$$

From eq 10a and 14a

$$k_0 = R_1 - k_2[B] \quad (15a)$$

Inserting [B] into eq 13a

$$k_0 = R_1 - k_2 \left(\frac{R_1}{k_2 + k_3[RX]} \right) \quad (16a)$$

$$k_0 = \frac{R_1 k_3 [RX]}{k_2 + k_3 [RX]} \quad (17a)$$

Inverting, we obtain

$$k_0^{-1} = \left(\frac{k_2}{R_1 k_3} \right) [RX]^{-1} + \left(\frac{1}{R_1} \right) \quad (6)$$

Registry No. 1a, 100927-74-0; 1b, 100927-75-1; 1c, 100927-76-2; 2a, 100927-77-3; 2b, 100927-78-4; 2c, 100927-79-5; $\text{Re}_2(\text{CO})_8(\mu\text{-cis-dppet})$, 100927-80-8; $\text{Re}_2(\text{CO})_8(\mu\text{-dppe})$, 100927-81-9; $\text{Re}_2(\text{CO})_8(\mu\text{-dpph})$, 100927-82-0; $(\mu\text{-H})\text{Re}_2(\text{CO})_8(\mu\text{-CH=CHC}_6\text{H}_5)$, 88294-19-3; $\text{Re}_2(\text{CO})_{10}$, 14285-68-8; $(\text{OC})_4\text{Re}(\mu\text{-dmpe})\text{Re}(\text{CO})_4$, 100927-83-1; $(\text{OC})_4\text{Re}(\mu\text{-dppe})\text{Re}(\text{CO})_4$, 100927-84-2; $(\text{OC})_4\text{Re}(\mu\text{-cis-dppet})\text{Re}(\text{CO})_4$, 100927-85-3; $(\text{OC})_4\text{Re}(\mu\text{-dpppe})\text{Re}(\text{OC})_4$, 100927-86-4; $(\text{OC})_4\text{Re}(\mu\text{-dpph})\text{Re}(\text{CO})_4$, 100927-87-5; THF, 109-99-9; CCl_4 , 56-23-5; CH_2Br_2 , 74-95-3; $\text{Re}(\text{CO})_4(\text{PPh}_2\text{Et})$, 100927-88-6; decaline, 14727-56-1; tetralin, 119-64-2; mesitylene, 108-67-8; toluene, 108-88-3; benzyl alcohol, 100-51-6; benzene, 71-43-2; acetonitrile, 75-05-8.

Complexation of Arenes by Macrocyclic Hosts in Aqueous and Organic Solutions¹

François Diederich,^{*2} Klaus Dick,³ and Dieter Griebel³

Contribution from the Department of Chemistry and Biochemistry, University of California, Los Angeles, California 90024, and the Max-Planck-Institut für medizinische Forschung, Abteilung Organische Chemie, D-6900 Heidelberg, Federal Republic of Germany.

Received October 11, 1985

Abstract: As spherical hosts for neutral arenes, the macrobicyclic compounds **2** and **3** were synthesized. 1-Acetyl-4,4-bis[4-succinimidylloxycarbonylmethoxy-3,5-dimethylphenyl]piperidine (**8**) and 1-ethyl-4,4-bis[4-(2-aminoethoxy)-3,5-dimethylphenyl]piperidine (**10**) were cyclized to the tetraoxadiaz[7.1.7.1]paracyclophane **4**. Cyclization component **8** was obtained by starting from 1-acetyl-4,4-bis(4-hydroxy-3,5-dimethylphenyl)piperidine and following the reaction sequence **6** → **7** → **8**. Compound **10** was obtained with use of the reaction sequence **8** → **9** → **10**. Reduction of **4** afforded 1',1''-diethyl-9,13,17,19,29,33,37,39-octamethylspiro[1,7,21,27-tetraoxa-4,24-diaza[7.1.7.1]paracyclophane-14,4':34,4''-bispiperidine] (**5**). **5** was cyclized with 1-benzoyloxycarbonyl-4,4-bis[chloroformylmethoxy-3,5-dimethylphenyl]piperidine (**12**), obtained by the reaction sequence **6** → **11** → **12**, to yield the macrobicyclic compound **13**. The advantages of amide macrocyclizations with *N*-hydroxysuccinimide esters as activated carboxylic acid derivatives are discussed. **13** was transformed into the target host **2** by following the sequence **13** → **14** → **2**. Host **3** was obtained by using the sequence **14** → **15** → **3** or by reduction of host **2**. Host **3**, 1',1'',1'''-triethyl-6,12,22,28,37,43,48,51,52,55,56,59-dodecamethyltrispiro[4,14,20,30,35,45-hexaoxa-1,17-diazaoctacyclo[15.15.15.2^{5,8}.2^{10,13}.2^{21,24}.2^{26,29}.2^{36,39}.2^{41,44}]nonapentaconta-5,7,10,12,21,23,26,28,36,38,41,43,48,50,52,54,56,58-octadecaene-9,4':25,4'':40,4''-trispiperidine], has *D*_{3h} symmetry. In host **3**, three diphenylmethane units bearing *N*-ethylpiperidine rings are attached each by two -O-CH₂-CH₂- chains to two cryptand-nitrogen atoms, through which the *D*_{3h} symmetry axis passes. In host **2**, one of the three diphenylmethane units is attached to the two nitrogens by two O-CH₂-C(O) bridges. The complexation between hosts **2** and **3** and neutral arenes in weakly acidic aqueous solution is studied. Association constants of the complexes were determined from solid-liquid and liquid-liquid extractions. The geometry of complexes in aqueous solution was elucidated by ¹H NMR spectroscopy. The considerable difference in binding, which was observed with the two very similar hosts **2** and **3**, is discussed. The first extensive study of the binding between neutral arenes and artificial macrocyclic hosts in various organic solvents of different polarity is presented. The complexation between arenes and hosts **2**, **3**, and **16** in organic solvents was monitored by electronic absorption and emission spectroscopy and ¹H NMR spectroscopy. Host **3** is a better binder for arenes in organic solvents than hosts **2** and **16**. Complexation between **3** and perylene, pyrene, or fluoranthene was even observed in benzene. The geometry of the complex of a specific host and a guest was found to be very similar in all solvents. The association constants of the complexes in organic solvents are discussed in terms of the contribution of attractive van der Waals interactions between host and guest in the complex and in terms of contributions of solvation-desolvation processes.

Artificial host-guest complexation in aqueous solution is closely related to complexation in biological systems and has attracted considerable interest during the past years.⁴ In order to investigate the interaction between apolar hosts and guests in aqueous solution, we have designed and synthesized water-soluble macromonocyclic hosts such as **1**.⁵⁻¹⁰ These compounds possess cavities of very

pronounced hydrophobic character as binding sites for apolar guests in aqueous solution. Extensive studies of binding by cyclodextrins¹¹ and by synthetic macrocycles in our⁵⁻¹⁰ and in other laboratories¹²⁻²¹ have definitely established that apolar hosts and

(1) This paper is dedicated to Prof. H. A. Staab on the occasion of his 60th birthday.

(2) University of California, Los Angeles.

(3) Max-Planck-Institut für medizinische Forschung, Heidelberg.

(4) For a recent review on host-guest complexation in aqueous solution, see: Diederich, F. *Nachr. Chem., Tech. Lab.* **1984**, *32*, 787-795.

(5) Diederich, F.; Dick, K. *Tetrahedron Lett.* **1982**, *23*, 3167-3171.

(6) Diederich, F.; Dick, K. *Angew. Chem., Int. Ed. Engl.* **1983**, *22*, 715-717; *Angew. Chem. Suppl.* **1983**, 957-972.

(7) Diederich, F.; Dick, K. *J. Am. Chem. Soc.* **1984**, *106*, 8024-8036.

(8) Diederich, F.; Griebel, D. *J. Am. Chem. Soc.* **1984**, *106*, 8037-8046.

(9) Diederich, F.; Dick, K.; Griebel, D. *Chem. Ber.* **1985**, *118*, 3588-3619.

(10) Diederich, F.; Dick, K. *Chem. Ber.* **1985**, *118*, 3817-3829.

(11) Bender, M. L.; Komiyama, M. "Cyclodextrin Chemistry"; Springer: Berlin, 1978.

(12) Murakami, Y. *Top. Curr. Chem.* **1983**, *115*, 107-159.

(13) Tabushi, I.; Yamamura, K. *Top. Curr. Chem.* **1983**, *113*, 145-182.

(14) Odashima, K.; Koga, K. In "Cyclophanes"; Keehn, P. M.; Rosenfeld, St. M., Eds.; Academic Press: New York, 1983; Vol. 2, pp 629-678.

(15) (a) Jarvi, E. T.; Whitlock, H. W. *J. Am. Chem. Soc.* **1982**, *104*, 7196-7204. (b) Miller, S. P.; Whitlock, H. W., Jr. *J. Am. Chem. Soc.* **1984**, *106*, 1492-1494.

(16) Winkler, J.; Coutouli-Argyropoulou, E.; Leppkes, R.; Breslow, R. *J. Am. Chem. Soc.* **1983**, *105*, 7198-7199.